Kulagina T. Yu., Sandrikov V. A.,
Van E. Yu., Zyabirova R. Z., Petrova Yu. N.
Scientific Institution "Petrovsky national research centre of surgery", Moscow, Russia

Evaluation of right and left ventricular function in patients with ischemic heart disease complicated by mitral insufficiency

Aim	To evaluate the right and left ventricular function and their interaction in patients with ischemic heart disease (IHD) complicated with mitral valve insufficiency (MVI) according to data of echocardiography (EchoCG) with the strain in gray scale, vector and diagram analyses.
Material and methods	The study included 118 patients evaluated with EchoCG at the preoperative stage of treatment; 71 of these patients had ischemic MVI (group 1) and 47 patients had uncomplicated IHD (group 2 or comparison group). Mean age of patients was 64±10 years. All patients underwent a surgery in an appropriate volume for myocardial revascularization supplemented with mitral valve plasty or replacement in patients with MVI. Standard EchoCG parameters and data obtained by postprocessing the EchoCG gray-scale images using the strain in gray scale, vector and diagram analyses were evaluated.
Results	In patients with complicated IHD, both global and local left ventricular (LV) systolic function and the right ventricular (RV) fractional area change (FAC) were significantly decreased. At the same time, there were no significant differences in the tricuspid annular plane systolic excursion (TAPSE) measured in M-mode and in the tricuspid annular systolic wave velocity (VSta), which also characterize the RV systolic function. The global longitudinal strain, the velocities of LV volume change and RV area change, and the long axis change velocity were informative for the right and left chambers, whereas the velocities of LV volume and RV area changes better detected RV disorders. The Pearson's correlation analysis used to identify the most significant parameters of interventricular interaction showed the presence of a strong inverse correlation, in the group of MVI patients, between the RV FAC and the degree of LV diastolic dysfunction (E/e') – r= –0,62; p=0.000, as well as the degree of MVI (vena contracta) – r= –0.58; p=0.001. In the comparison group of IHD patients without MVI, the correlation of RV FAC with E/e' was absent (r=0.28; p=0.192). The volume change velocity (dVol/dt) moderately correlated with the RV end-systolic and end-diastolic area in IHD patients but not in IHD patients with MVI. The RV area change velocity (dS/dt) evaluated during systole and diastole moderately significantly correlated with the LV end-diastolic volume.
Conclusion	Additional overload of left heart chambers in ischemic MVI is a factor that influences the development of the systemic and pulmonary circuit disorders. Recording and evaluation of global longitudinal strain, LV volume change velocity, and long axis change velocity with simultaneous recording of the segmental myocardial displacement velocity serve as highly informative criteria for disorders of LV and RV function. The vector analysis allows quantitative estimation of the local segmental myocardial function. Decreased velocities of the free RV wall segmental displacements during systole and diastole are characteristic of systolic and diastolic dysfunction in patients with IHD complicated with mitral regurgitation.

Keywords Ischemic mitral insufficiency; interventricular interaction; echocardiography

For citations Kulagina T. Yu., Sandrikov V. A., Van E. Yu., Zyabirova R. Z., Petrova Yu. N. Evaluation of right and left ventricular function in patients with ischemic heart disease complicated by mitral insufficiency. Kardiologiia. 2022;62(1):46–56. [Russian: Кулагина Т. Ю., Сандриков В. А., Ван Е. Ю., Зябирова Р. З., Петрова Ю. Н. Оценка функции правого и левого желудочков и взаимодействия между ними у пациентов с ишемической болезнью сердца, осложненной митральной недостаточностью. Кардиология. 2022;62(1):46–56].

Corresponding author Kulagina T. Yu. E-mail: takula@list.ru

Introduction

In developed economies, coronary artery disease (CAD) has long been a major cause of mortality. In the Russian Federation, cardiovascular diseases now play a leading role in all-cause mortality trends. According to the 2017 Russian Demographic Yearbook, cardiovascular deaths amounted to more than 50% of all-cause mortality [1]. In the same year, more than 6.5 million people in the Russian Federation had CAD, which was newly diagnosed in more than 1 million people [2]. Ischemic mitral valve insufficiency (MVI) develops in 20–25% of patients following acute myocardial infarction (MI) and in more

ISSN 0022-9040. Kardiologiia. 2022;62(1). DOI: 10.18087/cardio.2022.1.n1695

than 50% of patients with MI related heart failure (HF) [3, 4].

Patients with chronic MVI had more severe manifestations of HF and a less favorable prognosis than patients with uncomplicated CAD [5, 6].

Right ventricular (RV) dysfunction contributes substantially to the development of HF, both independently and in combination with left ventricular (LV) dysfunction. Moreover, isolated RV dysfunction has a less favorable prognosis than isolated LV dysfunction [7, 8]. Thus, early diagnosis of RV dysfunction becomes even more clinically relevant.

Objective

To evaluate RV and LV functions and their interaction in patients with CAD complicated by mitral valve dysfunction (MVI) using echocardiography with gray-scale strain imaging, vector and diagram analysis.

Material and Methods

The study included 118 patients with CAD, of whom 71 patients were 41 to 85 years old with CAD and a history of Q-wave MI later complicated by MVI (Group 1), while 47 patients were 45 to 83 years old with uncomplicated CAD (Group 2 or comparison group).

The study was approved by the ethics committee of the B. V. Petrovsky Russian Research Centre of Surgery (RRCS). All patients signed the informed consent to take part in the study, processing of the personal data and treatment results for further use in the prospective analysis.

Inclusion criteria were the following: CAD complicated by a history of Q-wave MI followed by moderate and severe MVI; CAD, uncomplicated course with hemodynamically significant involvement of two or more coronary arteries; satisfactory echolocation of the LV and RV myocardium; adequate frame rate in a dynamic range of ultrasound images (at least 50 frames per second).

Exclusion criteria were: connective tissue dysplasia (leaflet myxomatous degeneration, mitral valve (MV) prolapse, rupture of the anterior and/or posterior MV chordae); MC infective endocarditis; rheumatism; concomitant aortic valve defect; permanent and persistent atrial fibrillation, frequent ventricular and atrial premature beats and/or conduction disorders; MVI related with dilated cardiomyopathy due to mitral annulus ectasia; MVI associated with abnormal systolic motion of the anterior MV leaflet in hypertrophic cardiomyopathy.

The frequency of degenerative changes (mild leaflet thickening, fibrosis, small calcifications) in MV were nearly the same in both groups: 55 (78%) patients in Group 1 and 35 (75%) patients in Group 2.

The characteristics of the included patients are detailed in Table 1.

Selective coronary angiography showed that almost 50% of patients in both groups had multivessel CAD (46.8% and 44.7%, respectively). More than 50% involvement of the left coronary artery was also detected in both groups (38.2% and 52.5%, respectively). The right coronary artery (RCA) was involved in 100% of cases in patients with MVI. Q-wave MI affecting the LV posterior wall was diagnosed in 66.3% of cases, while 43.7% of patients had Q-wave MI of the LV inferior wall.

Arterial hypertension was diagnosed in 23 (32.4%) patients in Group 1 and 40 (85.1%) patients in Group 2.

Patients with uncomplicated CAD underwent various myocardial revascularization procedures. Myocardial revascularization was combined in patients with MVI with the reconstruction or replacement of MV; preservation methods were used in 63% of patients.

All patients underwent comprehensive transthoracic echocardiography prior to surgery under the protocol approved at the center and developed following the current guidelines of the Russian Society of Cardiology (RSC), the American Society of echocardiography (ASE) and the European Association of Cardiovascular Imaging (EACVI).

Echocardiography was performed using an expert-class Vivid-E9 (GE) device following a standard technique with simultaneous recording of one standard electrocardiographic (ECG) lead. The examination was conducted in gray-scale M-mode and two-dimensional mode using constant-wave, pulse-wave and color Doppler modes. The functional state of the heart was assessed by measuring the chamber geometry and the key indicators

Table 1. Characteristics of the included patients

Parameter	CAD with MVI (n=71)	CAD (n=47)
Demographics		
Age, years, M (SD)	64 (9)	62 (9)
Male, n (%)	53 (75)	40 (85)
Female, n (%)	18 (25)	7 (15)
CHF FC (NYHA), n (%)		
I	–	6 (13)
II	–	27 (57)
III	40 (56)	14 (30)
IV	31 (44)	–
Mitral valve insufficiency grade, n (%)		
1	–	39 (83)
2	18 (25)	8 (17)
3	44 (62)	-
4	9 (13)	–

CAD – coronary artery disease;
MVI – mitral valve insufficiency;
FC – functional class; CHF – chronic heart failure.

of central hemodynamics: volumetric measures of the heart chambers, parameters of the blood flow velocity and pressure in the pulmonary circulation. Left ventricular end-systolic volume (LVESV) and end-diastolic volume (LVEDV), as well as left ventricular ejection fraction (LVEF), were obtained using the method of disks (modified Simpson's rule); LV contractility was assessed by calculating the LV local contractility index (LCI). The degree of MVI was assessed by several echocardiographic parameters, including the radius of the proximal isovelocity surface area (PISA), vena contracta, volume, and fraction of regurgitation [9]. LV diastolic function was estimated following the 2016 ASE/EACVI Guideline for the Evaluation of Left Ventricular Diastolic Function by Echocardiography [10].

Left atrial volume (LAV) was measured from the apical four-chamber and two-chamber views at the ventricular end-systole. Right atrial volume (RAV) was measured from the apical four-chamber view at the ventricular end-systole.

Some geometric indicators were indexed to the body surface area (BSA) following the Russian guidelines for measurement of the heart chambers and taking into consideration the anthropometric differences within the sample.

Right ventricular fractional area change (RVFAC) was measured from the apical four-chamber view. RVFAC was calculated by measuring RV end-systolic are (RVESA) and end-diastolic area (RVEDA), for which the RV endocardium was mapped from the edge of the fibrous tricuspid annulus, along the RV free wall endocardium, to the apex, and back to the fibrous annulus along the interventricular septal (IVS) endocardium, both at end-systole and end-diastole. Moreover, tricuspid annular plane systolic excursion (TAPSE) was obtained in the M-mode, while the fibrous tricuspid annulus systolic wave velocity (FTA Vs) was determined in pulsed wave tissue Doppler mode to assess the systolic function of the RV.

RV diastolic function was estimated by the peak early (E) and late (A) RV filling velocities when studying the TV flow in the pulsed wave Doppler mode; the movement of the fibrous tricuspid annulus (peak early diastole E') was evaluated using the tissue Doppler mode [11]. The mean pulmonary artery pressure (mPAP) was determined by the systolic pulmonary artery flow times in the continuous wave Doppler mode (Kitabatake).

Static and dynamic images of the three cardiac cycles were stored in the Echopac 7 (GE) workstation. LV and RV strain was assessed using gray-scale strain imaging. Grayscale RV and LV cineloops were stored in the DICOM file format and exported to the database on a personal computer to be analyzed in a software program developed by the RRCS Department of Instrumental and Radiation Diagnosis [12, 13].

The four-chamber apical view was used for the processing and analysis, which allowed both ventricles to be visualized and analyzed simultaneously. The program allows simultaneously processing LV and RV findings and obtaining data on cardiac performance at one cardiac cycle. Thus, the following images were obtained in a semi-automatic interactive mode after ventricular endocardium mapping: IVS, LV lateral wall and RV free wall myocardial displacement velocity (Figure 1). LV was divided into 6 segments (3 lateral wall segments and 3 IVS segments), while RV was divided into 4 segments (2 free wall segments and 2 IVS segments).

Following vector analysis (one cardiac cycle), the following generalizing diagrams were constructed: flow-volume for LV that linked the volume and rate of volume change over time; flow-area for RV that linked area and area change over time, which allowed assessing the global ventricular function. The following parameters were calculated automatically using the flow-volume diagram: LVESV and LVEDV; LV volume change rate (dVol/dt) in systole (s) and diastole (d); LV long axis change rate (dLA/dt) in systole (s) and diastole (d); sum of normal LV myocardial displacement velocities, sum of Vn in systole (s) and diastole (d). The following parameters were derived from the flow-area diagram: RVESA; RVEDA; rate of RV area change (dS/dt) in systole (s) and diastole (d); rate of RV long axis change (dLA/dt) in systole (s) and diastole (d); sum of normal RV flow velocities; sum of Vn in systole (s) and diastole (d).

The flow-volume diagrams for LV and the flow-area diagrams are fully consistent with the phase structure of the cardiac cycle (Figure 2).

Since vector analysis allows local contractility to be quantified, the diagram method can be used to estimate global systolic and diastolic functions of RV and LV.

Statistical processing of the data obtained was performed in Statistica 10.0 using commonly used statistical methods and the determination of the main quantitative characteristics: mean and standard deviation (M±SD), the median and interquartile range (Me [25^{th} percentile; 75^{th} percentile]). Normally distributed quantitative traits were compared using Student's t-test, while Kruskal – Wallis analysis of variance was used in the non-normal distribution. After performing correlation analysis, the bivariate Pearson correlation coefficients (r) were calculated to show the correlations between the characteristics of interest and the observation data. The differences were statistically significant with p value less than 0.05.

Results

Analysis of the key hemodynamic and echocardiographic parameters (Table 2) showed that patients with complicated

ISSN 0022-9040. Kardiologiia. 2022;62(1). DOI: 10.18087/cardio.2022.1.n1695

Figure 1. Left and right ventricular myocardial displacement velocity vectors (A) and graphical representation of left ventricular displacement velocity (B) and right ventricular displacement velocity (C); electrocardiographic curve (D)

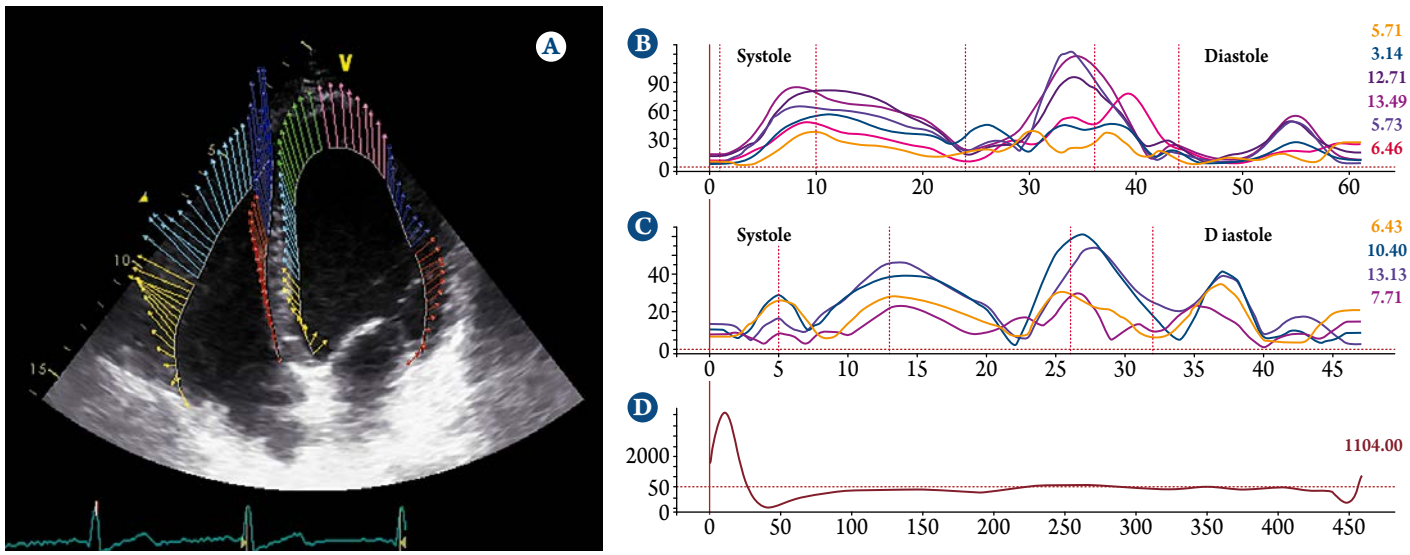

The colors of the vectors in Figure 1, A corresponds to the colors of the curves in Figure 1, B and Figure 1, C; the red vertical marker (B, C, D) corresponds to the phase of isovolumic contraction; the white vertical line on the diagrams (B, C) indicates a phase of the cardiac cycle according to the electrocardiogram (D). The other explanations are provided in the text.

CAD had statistically significantly lower systolic and diastolic blood pressure (BP). As confirmed by reduced LVEF and increased LCI, the global decrease in local LV systolic function was statistically significant in such patients. Hemodynamically significant volume overload of the left heart ventricle in MVI is an additional factor for increased LV and RV volumes. LV and RV volumes, including those indexed to BSA, were statistically significantly higher in the group of patients with CAD complicated with MVI. Increased LA volume and elevated LA pressure are the direct result of chronic MVI. Increased LA pressure leads to pulmonary hypertension (PH) gradually and indirectly via the pulmonary circulation.

Our patients with MVI had statistically significantly increased mPAP. PH developing in the decreased LV systolic function and secondary MVI increases RV afterload, contributing to its dysfunction of varying severity.

Figure 2. Left ventricular flow-volume diagram and flow-area diagram in uncomplicated coronary artery disease

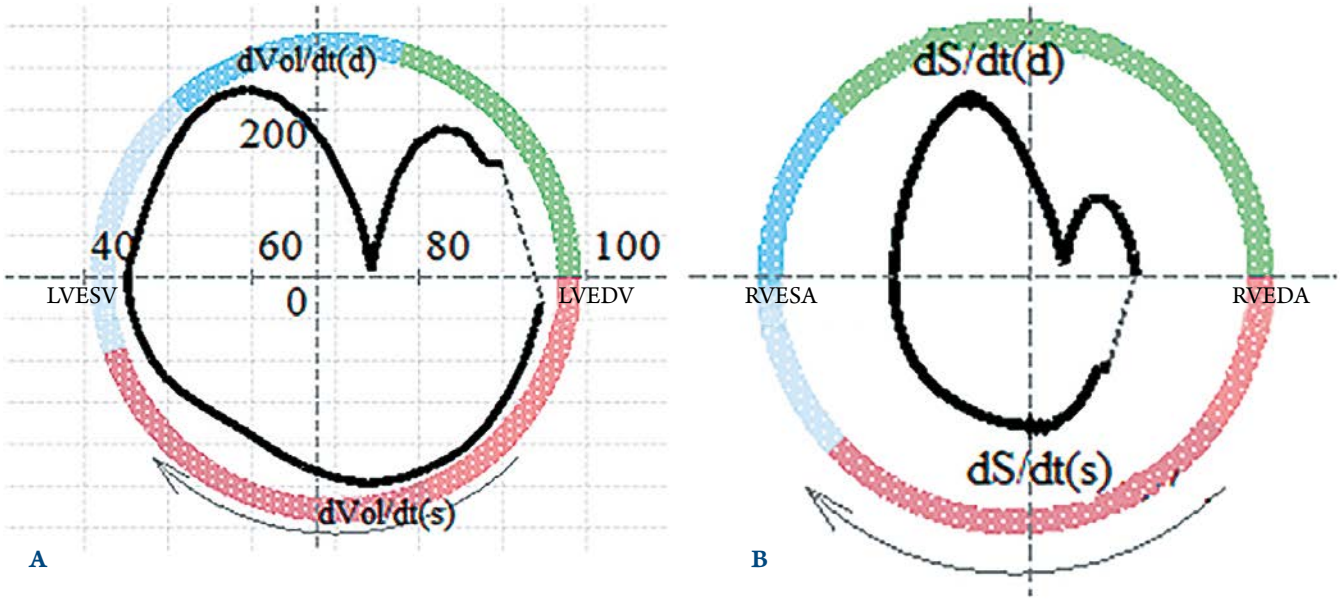

A – LV flow-volume diagram: horizontal axis – LV volume in milliliters, vertical axis – velocity in milliliters per second; B – RV flow-area diagram: horizontal velocity – RV area in square centimeters; vertical axis – velocity in square centimeters per second. LVESV, left ventricular end-systolic volume.

While patients with MVI have statistically significantly reduced RVFAC, no statistically significant differences have been recorded between TAPSE and FTA Vs that also describe the systolic RV function. Thus, it is a relevant and important task to search for new indicators for diagnosing and predicting RV dysfunction.

Pearson's correlation analysis, which used to find the most significant parameters of interventricular interaction, showed that there was a strong two-way correlation of RVFAC with the degree of LV diastolic dysfunction (E/e') (r=–0.62; p=0.000) and the degree of MVI (vena contracta) (r=–0.58; p=0.001) CAD in patients with MVI. There was no correlation between RVFAC and E/e' in the comparison group of CAD patients without MVI (r=0.28; p=0.192).

A comparison of LV and RV diastolic dysfunction in the study samples is presented in Table 3.

Patients with uncomplicated CAD had mainly LV diastolic dysfunction type 1, while patients with MVI had mainly type 2. Although RV diastolic dysfunction type 1 prevailed in almost the same percentage of cases in both groups, severe diastolic dysfunction of both ventricles was observed only in 3% of patients with complicated CAD.

The results of gray-scale two-dimensional strain imaging used to obtain new parameters for diagnosing RV dysfunction and selecting additional precise assessment methods for interventricular interaction are presented in Table 4 along with vector and diagram analyses. The novel methods for assessing systolic and diastolic ventricular function detected a statistically significant deterioration in several parameters characterizing LV and RV in patients with complicated CAD. Global longitudinal strain, LV volume and RV area change rates, and long axis change rate were informative for the left and right heart ventricles; the segment displacement velocities detected RV abnormalities more accurately.

The operational diagrams resulting from the post-processing of two-dimensional echocardiographic images of RV clearly show the identified differences between the patient groups (Figure 3).

The most significant change in the curve in diastole (flattening, peak smoothing) observed in one patient with MVI (Figure 3, A) reflects diastolic RV dysfunction; here, the curve in the systole is sharper and deeper than that obtained in a patient with CAD (Figure 3, B), which may be indicative the presence of severe TV regurgitation and RV volume overload in complicated CAD. Thus, patients with CAD and MVI have both RV systolic and diastolic dysfunction.

Vector analysis can be used to quantify the local function of RV segments per cardiac cycle. The diagram of the RV displacement velocities (Figure 4) clearly shows a severe decrease in the displacement velocities of the RV free wall segments in systole and diastole, as well as the mismatch of the displacement velocity peaks in systole and the absence of two peaks in diastole. This is indicative of the RV systolic and diastolic dysfunction in patients with CAD and MVI compared to those with uncomplicated CAD.

The evaluation of the interventricular interaction using new parameters of myocardial function and correlation analysis revealed the patterns shown in Table 5. Here, the left (GSmean) and right (LStotal) ventricular strain parameters were not statistically significantly correlated

Table 2. Basic hemodynamic and echocardiographic parameters in patients with CAD complicated by MVI compared to patients with uncomplicated CAD

Parameter	CAD with MVI (n=71)	CAD (n=47)	p
Hemodynamic parameters			
HR, bpm	71±14	66±9	0.173
SBP, mm Hg	112±17	136±19	<0.0001
DBP, mm Hg	71±9	80±11	0.0006
Left heart			
LVEDV, mL	144±37	88±19	<0.0001
LVEDVI, mL/m^2	75±17	44±8	<0.0001
LVESV, mL	80±31	32±9	<0.0001
LVEF, %	46±10	63±4	<0.0001
LCI	1.7±0.4	1.0±0	<0.0001
LA volume, mL	85±24	67±15	0.002
LAVI, mL/m^2	45±14	34±7	0.001
Right heart			
RVEDA, cm^2	20±7	17±4	0.089
RVEDAI, cm^2/m^2	10±3	9±1	0.047
RVESA, cm2	13±6	11±2	0.034
RVESAI, cm2/m^2	7±2	5±1	0.012
TAPSE, mm	19±4	21±2	0.137
FTA Vs, cm/s	15±2	14±2	0.327
RVFAC	35±9	40±6	0.015
RAV, mL	50±20	43±12	0.181
RAVI, mL/m^2	27±12	22±6	0.120
mPAP, mm Hg	30±12	14±4	<0.0001

The data are presented as the mean and standard deviation (M±SD); MVI – mitral valve insufficiency; HR – heart rate; SBP – systolic blood pressure; DBP – diastolic blood pressure; LVEDV – left ventricular end-diastolic volume; LVESV – left ventricular end-systolic volume; LVEF – left ventricular ejection fraction; LCI – local contractility index; LAV – left atrial volume; RVEDA – right ventricular end-diastolic area; RVESA – right ventricular end systolic area; TAPSE – tricuspid annular plane systolic excursion; FTA Vs – fibrous tricuspid annulus systolic wave velocity; RVFAC – right ventricular fractional area change; RAV – right atrial volume; mPAP – mean pulmonary artery pressure.

ISSN 0022-9040. Kardiologiia. 2022;62(1). DOI: 10.18087/cardio.2022.1.n1695

Table 3. Diastolic function of the left and right ventricles

Parameter	CAD with MVI (n=71)	CAD (n=47)
Left ventricle, n (%)		
Normal function	–	–
Dysfunction type 1	30 (42)	41 (87)
Dysfunction type 2	39 (55)	6 (13)
Dysfunction type 3	2 (3)	–
Right ventricle, n (%)		
Normal function	–	2 (4)
Dysfunction type 1	40 (56)	29 (62)
Dysfunction type 2	29 (41)	16 (34)
Dysfunction type 3	2 (3)	–

CAD – coronary artery disease; MVI – mitral valve insufficiency.

with the geometric and functional parameters of the opposite ventricles.

The integral index of LV systolic and diastolic functions calculated as volume change rate (dVol/dt) was moderately correlated with the RV end-systolic and end-diastolic areas in patients with CAD and MVI; such correlation was absent in the comparison group. There was statistically significant moderate correlation between RV area change rate (dS/dt) in systole and diastole and LVEDV in both study groups. These encouraging findings underline the importance of finding new parameters of ventricular interaction using new methods of assessing myocardial function.

Discussion

Evaluating the RV function is of the utmost diagnostic importance. A number of researchers have used echocardiographic evaluation of the strain to figure out the extent of RV myocardial involvement in a particular disease. According to Hutyra et al. [14], it is reasonable to use RV longitudinal strain (LSfr) along with data on hemodynamic instability and ECG when assessing RV myocardial scarring following acute inferior ST segment elevation MI and subsequent stenting of infarct-related RCA. The authors distinguished three groups of patients depending on the RV LSfr values: Group 1 – normal strain (RV LSfr < –20%); Group 2 – hibernating myocardium (baseline RV LSfr > –20%, on day 5 after stenting RV LSfr < –20%); Group 3 – RV scarring (RV LSfr remains > –20%). RV LSfr > –15.8% showed the sensitivity of 92% and specificity of 83% in predicting RV scarring (AUC=0.93). The presence of myocardial scarring was verified by gadolinium-enhanced magnetic resonance imaging conducted one month after implanting a bare-metal stent. The authors also point out in this paper that RV LSfr is superior to TAPSE and TVI in detecting RV scarring. This is consistent with our findings: TAPSE and TVI (FTA Vs) did not reveal differences between the study groups. The indicators of RV myocardial strain presented by Hutyra et al. [14] agree with our results. RV LSv was less than –20% (– 21.8±3.5%) in the group of patients with uncomplicated CAD; the strain significantly decreased to –15.9±6.5% in the group of patients with CAD complicated with MVI. This is confirmed by the vector analysis conducted to estimate the function of the RV segments. Here, the severe decrease in the contraction velocities of the RV free lateral wall segments in systole and

Table 4. Vector analysis, diagram method, and strain rates in patients with uncomplicated and complicated CAD

Parameter	CAD with MVI (n=71)	CAD (n=47)	p
Left ventricle			
GS4k	–11.6±3.6	–17.2±2.2	<0.0001
GS2k	–11.5±3.7	–17.1±2.0	<0.0001
GS mean	–11.5±3.5	–17.2±1.9	<0.0001
dVol/dt (s), cm3/s	250±65	191±36	<0.0001
dVol/dt (d), cm3/s	263±80	183±28	<0.0001
dLA/dt (s), mm/s	46±14	55±11	0.016
dLA/dt (d), mm/s	48±14	55±10	0.035
Sum Vn (s), mm/s	18.2±4.9	18.7±3.3	0.616
Sum Vn (d), mm/s	19.3±6.8	18.2±3.4	0.466
Right atrium			
RVLSfr	–15.9±6.5	–21.8±3.5	0.0001
RVLStot	–15.4±4.4	–18.6±2.3	0.002
dS/dt (s), cm2/s	26±10	32±11	0.045
dS/dt (d), cm2/s	27±13	32±8	0.112
dLA/dt (s), mm/s	71±25	79±19	0.212
dLA/dt (d), mm/s	72±27	73±24	0.872
Sum Vn (s), mm/s	8.7±5.2	14.1±5.7	0.0003
Sum Vn (d), mm/s	8.3±5.9	15.5±6.9	<0.0001
V1 (s), mm/s	30.0 [19.2; 36.7]	31.9 [22.4; 39.8]	0.191
V2 (s), mm/s	20.8 [13.7; 26.2]	24.8 [20.2; 25.4]	0.043
V3 (s), mm/s	20.4 [14.6; 26.3]	27.9 [24.0; 31.0]	0.003
V4 (s), mm/s	19.0 [14.8; 26.7]	27.3 [21.3; 32.2]	0.007
V1 (d), mm/s	27.4 [18.3; 34.5]	34.4 [25.2; 40.6]	0.034
V2 (d), mm/s	17.6 [11.3; 25.0]	28.8 [23.4; 29.5]	<0.0001
V3 (d), mm/s	18.3 [14.0; 27.3]	28.1 [23.6; 30.6]	0.004
V4 (d), mm/s	18.5 [12.3; 27.5]	30.7 [26.5; 33.4]	<0.0001

Normally distributed quantitative data are presented as M ± SD; other data are expressed as Me [25th percentile; 75th percentile].
CAD – coronary artery disease; MVI – mitral valve insufficiency.

ISSN 0022-9040. Kardiologiia. 2022;62(1). DOI: 10.18087/cardio.2022.1.n1695

Figure 3. Right ventricular flow-area diagram

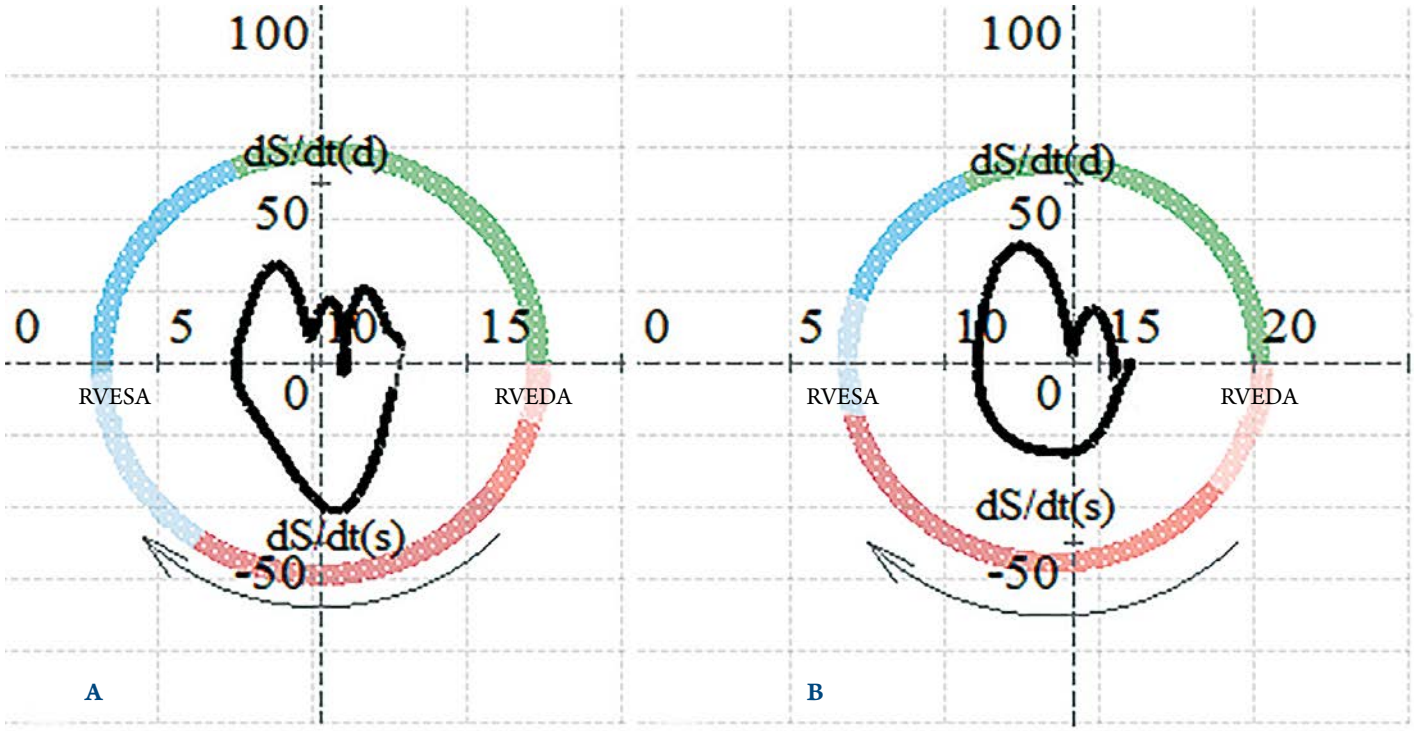

A – in coronary artery disease complicated with mitral valve insufficiency; B – in uncomplicated coronary artery disease. Horizontal axis – right ventricular area, cm2; vertical axis – area change rate, cm^2/s. Above the horizontal axis – diastole, under the horizontal axis – systole. RVESA, right ventricular end-systolic area.

diastole, dyssynchronous contraction of the segments in systole and absence of two peaks in diastole is indicative of the RV systolic and diastolic dysfunction in patients with CAD and MVI. This can be a sign of the pathological involvement of a certain segment of the RV myocardium and the formation of foci of fibrosis in complicated CAD, which is manifested later by the abnormal mechanics of RV contraction and relaxation.

In their study focusing on the deformation properties of the LV myocardium and papillary muscles in patients with MVI, Buziashvili et al. [15] used tissue doppler imaging (TDI) to study the myocardium. Longitudinal systolic strain of all LV walls of interest were also reduced in the group of CAD patients without MVI compared to normal walls, but to a lesser extent than in patients with MVI. This is consistent to our findings for the parameters of LV myocardial function assessed by gray-scale strain imaging and vector analysis.

Structural and functional abnormalities occur in the myocardium due to a variety of causes, such as direct damage to the myocardium and/or connective tissue structures, coronary artery insufficiency, volume and pressure overload, as well as development of hypertrophy [16]. However, it is important to understand that remodeling processes only affect LV or IVS. While RV is almost always involved, this is an understudied and complex diagnostic task [17]. The study by Loskutova et al. [18] further developed the concept of interventricular interaction expressed in the mutual influence of wall motion, ventricular preload and post-load, ventricular interrelation and interdependence in systole and diastole. Using the gray-scale two-dimensional strain

Table 5. Results of the correlation analysis

Parameter	Group	RVEDAI	RVESAI	LVEDV
dVol/dt(s)	CAD with MVI	r=0.63 p=0.000	r=0.60 p=0.001	–
	CAD	r= –0.16 p=0.46	r= –0.26 p=0.23	–
dVol/dt(d)	CAD with MVI	r=0.62 p=0.000	r=0.56 p=0.002	–
	CAD	r= –0.26 p=0.23	r= –0.34 p=0.11	–
dS/dt(s)	CAD with MVI	–	–	r=0.42 p=0.025
	CAD	–	–	r=0.51 p=0.014
dS/dt(d)	CAD with MVI	–	–	r=0.45 p=0.015
	CAD	–	–	r=0.46 p=0.027

CAD – coronary artery disease; MVI – mitral valve insufficiency – LVEDV – left ventricular end-diastolic volume; RVEDAI – right ventricular end-diastolic area index; RVESAI – right ventricular end-systolic area index; dVol/dt – integral index of LV systolic and diastolic function calculated as volume change rate in systole (s) and diastole (d); dS/dt – RV area change rate in systole (s) and diastole (d).

Figure 4. Right ventricular myocardial displacement velocity diagrams synchronized with electrocardiogram (bottom) per cardiac cycle

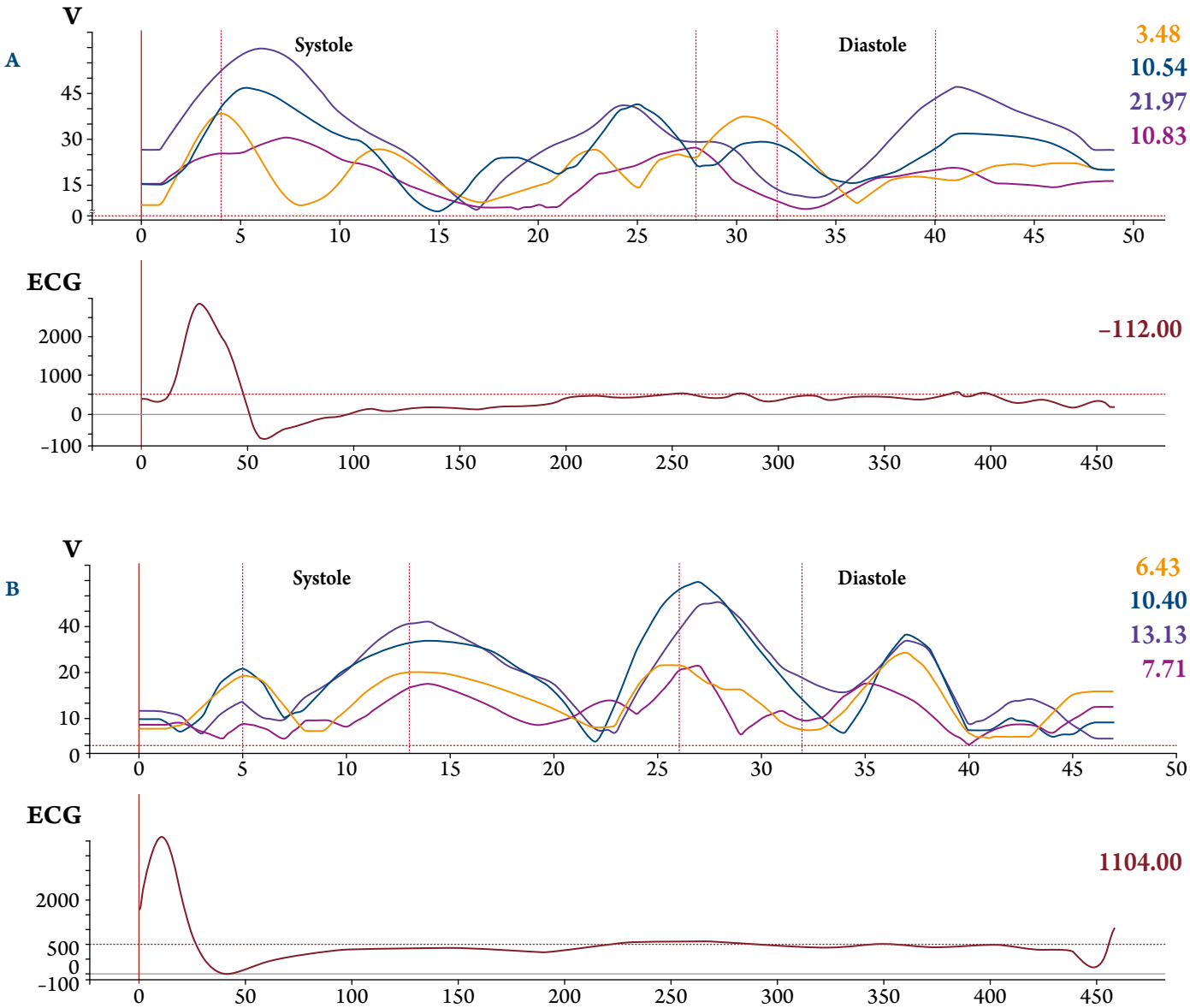

A – in coronary artery disease complicated with mitral valve insufficiency;
B – in uncomplicated coronary artery disease. Colors of the curves correspond to the colors of the right ventricular segments in Figure 1.

imaging to study the involvement of RV in the pathological process in hypertensive heart disease (HHD), the authors discovered that RV free wall deformation was –28.7±5.3% in healthy individuals, but lower in patients with HHD grade 3 (– 24.5±7.9%). However, these values were higher in both groups than in our patients with CAD. Coronary insufficiency may have a more pronounced effect on the myocardium and its strain. According to the authors, the IVS-mediated hemodynamic effect of LV in increased post-load may be a possible mechanism of RV dysfunction in HHD. As we noted earlier, the involvement of RCA is often accompanied by ischemic damage to RV, which worsens the prognosis in these patients. Thus, searching for parameters to determine the degree of RV damage remains a relevant cardiologic task.

The most commonly used parameters today are tricuspid annular plane systolic excursion (TAPSE) determined in the M-mode and the fibrous tricuspid annulus systolic wave velocity (FTA Vs) determined in the pulsed wave tissue Doppler mode. The values of FTA Vs for the diagnosis of RV dysfunction differ between researchers: 11.1 cm/s with the sensitivity of 86% and specificity of 98% [19]; <11.5 cm/s with the sensitivity of 90% and specificity of 85% [20]; <12 cm/s with the sensitivity of 81% and specificity of 82% [21]; 13 cm/s with the sensitivity of 89% and specificity of 71% [22]. However, all these values are lower than in our study (14 cm/s). Nevertheless, it should be noted that almost all studies included patients who had a history of MI in the

ISSN 0022-9040. Kardiologiia. 2022;62(1). DOI: 10.18087/cardio.2022.1.n1695

RCA area with the involvement of RV. Alam et al. [23] presented the data on RV function in patients with inferior MI compared to healthy individuals and patients with anterior MI. TAPSE was significantly lower in patients with history of MI than healthy individuals (20.5 mm and 25 mm, respectively; $p < 0.001$). This study agrees well with our findings that TAPSE was decreased in patients with CAD (regardless of the presence or absence of a history of Q-wave MI) (19 mm and 21 mm, respectively; $p>0.137$).

Conclusion

Additional volume overload of the left heart in ischemic mitral valve insufficiency is a factor affecting the development of disorders of the systemic and pulmonary circulation. Registration and estimation of the global longitudinal strain, left ventricular volume change rate, as well as long axis change rate and simultaneous registration of the myocardial segment displacement velocity, are highly informative criteria for assessing the left and right ventricular dysfunction. Vector analysis allows the local function of myocardial segments to be quantified. Decreased displacement velocity of the free wall segments of the right ventricle in systole and diastole is characteristic of systolic and diastolic dysfunction in patients with coronary artery disease complicated with mitral regurgitation.

Funding

The study was performed a part of the State Assignment of the Academician B.V. Petrovsky National Research Centre of Surgery # 0394-2020-0007 «Creation of the Informational Platform for Support of Decision-Making in Diagnostics and Treatment of Patients with Pathologies of the Cardiovascular System and Oncology».

No conflict of interest is reported.

The article was received on 20.05.2021

REFERENCES

1. Federal State Statistics Service. Russain Statistical Yearbook 2018. Av. at: https://rosstat.gov.ru/storage/mediabank/year18.pdf. -M.: Rosstat;2018. - 694 p. [Russian: Федеральная служба государственной статистики. Российский статистический ежегодник. 2018. – М.:Росстат; 2018. - 694с. Доступно на: https://rosstat.gov.ru/storage/mediabank/year18.pdf]. ISBN 978-5-89476-456-6
2. Ministry of Health of Russian Federation. Statistical compendium 2018. Morbidity of the entire population of Russia. Av. at: https://minzdrav.gov.ru/ministry/61/22/stranitsa-979/statisticheskie-i-informatsionnye-materialy/statisticheskiy-sbornik-2018-god. [Russian: Министерство здравоохранения Российской Федерации. Статистический сборник 2018. Заболеваемость всего населения России. Доступно на: https://minzdrav.gov.ru/ministry/61/22/stranitsa-979/statisticheskie-i-informatsionnye-materialy/statisticheskiy-sbornik-2018-god]
3. Di Bella G, Siciliano V, Aquaro GD, De Marchi D, Rovai D, Carerj S et al. Right ventricular dysfunction: an independent and incremental predictor of cardiac deaths late after acute myocardial infarction. The International Journal of Cardiovascular Imaging. 2015;31(2):379–87. DOI: 10.1007/s10554-014-0559-9
4. Piccolo R, Niglio T, Spinelli L, Capuano E, Strisciuglio T, D'Anna C et al. Reperfusion Correlates and Clinical Outcomes of Right Ventricular Dysfunction in Patients With Inferior ST-Segment Elevation Myocardial Infarction Undergoing Percutaneous Coronary Intervention. The American Journal of Cardiology. 2014;114(2):243–9. DOI: 10.1016/j.amjcard.2014.04.034
5. Rossi A, Dini FL, Faggiano P, Agricola E, Cicoira M, Frattini S et al. Independent prognostic value of functional mitral regurgitation in patients with heart failure. A quantitative analysis of 1256 patients with ischaemic and non-ischaemic dilated cardiomyopathy. Heart. 2011;97(20):1675–80. DOI: 10.1136/hrt.2011.225789
6. Asgar AW, Mack MJ, Stone GW. Secondary Mitral Regurgitation in Heart Failure. Journal of the American College of Cardiology. 2015;65(12):1231–48. DOI: 10.1016/j.jacc.2015.02.009
7. Korabathina R, Heffernan KS, Paruchuri V, Patel AR, Mudd JO, Prutkin JM et al. The pulmonary artery pulsatility index identifies severe right ventricular dysfunction in acute inferior myocardial infarction. Catheterization and Cardiovascular Interventions. 2012;80(4):593–600. DOI: 10.1002/ccd.23309
8. Grothoff M, Elpert C, Hoffmann J, Zachrau J, Lehmkuhl L, de Waha S et al. Right Ventricular Injury in ST-Elevation Myocardial Infarction: Risk Stratification by Visualization of Wall Motion, Edema, and Delayed-Enhancement Cardiac Magnetic Resonance. Circulation: Cardiovascular Imaging. 2012;5(1):60–8. DOI: 10.1161/CIRCIMAGING.111.967810
9. Lancellotti P, Tribouilloy C, Hagendorff A, Popescu BA, Edvardsen T, Pierard LA et al. Recommendations for the echocardiographic assessment of native valvular regurgitation: an executive summary from the European Association of Cardiovascular Imaging. European Heart Journal - Cardiovascular Imaging. 2013;14(7):611–44. DOI: 10.1093/ehjci/jet105
10. Nagueh SF, Smiseth OA, Appleton CP, Byrd BF, Dokainish H, Edvardsen T et al. Recommendations for the evaluation of left ventricular diastolic function by echocardiography: an update from the American Society of Echocardiography and the European Association of Cardiovascular Imaging. Journal of the American Society of Echocardiography. 2016;29(4):277–314. DOI: 10.1016/j.echo.2016.01.011
11. Rudski LG, Lai WW, Afilalo J, Hua L, Handschumacher MD, Chandrasekaran K et al. Guidelines for the Echocardiographic Assessment of the Right Heart in Adults: A Report from the American Society of Echocardiography. Journal of the American Society of Echocardiography. 2010;23(7):685–713. DOI: 10.1016/j.echo.2010.05.010
12. Sandrikov V.A., Kulagina T.Yu, Vardanyan A.A., Gavrilov A.V., Arkhipov I.V. New Approach to Assessment of Systolic and Diastolic Function of Left Ventricle Diastolic and Systolic Functions in Patients with Coronary Heart Disease. Ultrasound and Functional Diagnostics. 2007;1:44–54. [Russian: Сандриков В.А., Кулагина Т.Ю., Варданян А.А., Гаврилов А.В. Архипов И.В. Новый подход к оценке систолической и диастолической функции левого желудочка у больных с ишемической болезнью сердца. Ультразвуковая и функциональная диагностика. 2007;1:44-54]
13. Kulagina T.Yu., Belenkov Yu.N., Sandrikov V.A. New Algorithms for Evaluation Myocardial Function According to Echocardiography. Kardiologiia. 2019;59(11):48–55. [Russian: Кулагина Т.Ю., Беленков Ю.Н., Сандриков В.А. Новые алгоритмы оценки функции миокарда по данным эхокардиографии. Кардиология. 2019;59(11):48-55]. DOI: 10.18087/cardio.2019.11.10273
14. Hutyra M, Skála T, Horák D, Köcher M, Tüdös Z, Zapletalová J et al. Echocardiographic assessment of global longitudinal right ventricular function in patients with an acute inferior ST elevation myocardial infarction and proximal right coronary artery occlusion. The International Journal of Cardiovascular Imaging. 2015;31(3):497–507. DOI: 10.1007/s10554-014-0573-y

15. Buziashvili Yu.I., Koksheneva I.V., Asymbekova E.U., Turakhonov T.K. Left ventricular and papillary muscles deformation in patients with coronary artery disease and ischemic mitral regurgitation. Cardiology and Cardiovascular Surgery. 2019;12(2):100–9. [Russian: Бузиашвили Ю.И., Кокшенева И.В., Асымбекова Э.У., Турахонов Т.К. Деформация миокарда левого желудочка и папиллярных мышц митрального клапана у больных с ишемической болезнью сердца и ишемической митральной регургитацией. Кардиология и сердечно-сосудистая хирургия. 2019;12(2):100-9]. DOI: 10.17116/kardio201912021100
16. Sandrikov V.A., Kulagina T.Yu., Van E.Yu. Myocardial dysfunction. Adaptation and de-adaptation of the heart. In: Ultrasound and radiation technologies in clinical practice. - 2012;M.: STROM:71–83. [Russian: Сандриков В.А., Кулагина Т.Ю., Ван Е.Ю. Дисфункция миокарда. Адаптация и деадаптация сердца. В сборнике: Ультразвуковые и лучевые технологии в клинической практике. – М.: СТРОМ, 2012. С.71–83]
17. Berezina E.V., Kulagina T.Yu., Van E.Yu., Sandrikov V.A. Modern echocardiographic methods of right ventricle assessment. Ultrasound and radiation technologies in clinical practice. - 2012;M.: STROM:45–54. [Russian: Березина Е.В., Кулагина Т.Ю., Ван Е.Ю., Сандриков В.А. Современные эхокардиографические методы оценки правого желудочка. В сборнике: Ультразвуковые и лучевые технологии в клинической практике. - М.: СТРОМ, 2012. - С.45-54]
18. Loskutova A.S., Saidova M.A., Shitov V.N., Rogoza A.N. Echocardiographic assessment of right ventricular dysfunction versus left ventricular dysfunction in patients with hypertension. Russian Heart Journal. 2013;12(5):316–23. [Russian: Лоскутова А. С., Саидова М. А., Шитов В. Н., Рогоза А. Н. Эхокардиографическая оценка дисфункции правого желудочка сердца в сравнении с левым у пациентов с гипертонической болезнью. Сердце: журнал для практикующих врачей. 2013;12(5):316-23]
19. Kidawa M, Chizynski K, Zielinska M, Kasprzak JD, Krzeminska-Pakula M. Real-time 3D echocardiography and tissue Doppler echocardiography in the assessment of right ventricle systolic function in patients with right ventricular myocardial infarction. European Heart Journal - Cardiovascular Imaging. 2013;14(10):1002–9. DOI: 10.1093/ehjci/jes321
20. Meluzín J, Spinarová L, Bakala J, Toman J, Krejcí J, Hude P et al. Pulsed Doppler tissue imaging of the velocity of tricuspid annular systolic motion. A new, rapid, and non-invasive method of evaluating right ventricular systolic function. European Heart Journal. 2001;22(4):340–8. DOI: 10.1053/euhj.2000.2296
21. Ozdemir K, Altunkeser BB, Ićli A, Ozdil H, Gok H. New Parameters in Identification of Right Ventricular Myocardial Infarction and Proximal Right Coronary Artery Lesion. Chest. 2003;124(1):219–26. DOI: 10.1378/chest.124.1.219
22. Witt N, Alam M, Svensson L, Samad BA. Tricuspid Annular Velocity Assessed by Doppler Tissue Imaging as a Marker of Right Ventricular Involvement in the Acute and Late Phase after a First ST Elevation Myocardial Infarction. Echocardiography. 2010;27(2):139–45. DOI: 10.1111/j.1540-8175.2009.00985.x
23. Alam M, Wardell J, Andersson E, Samad BA, Nordlander R. Right ventricular function in patients with first inferior myocardial infarction: assessment by tricuspid annular motion and tricuspid annular velocity. American Heart Journal. 2000;139(4):710–5. DOI: 10.1016/s0002-8703(00)90053-x

ISSN 0022-9040. Kardiologiia. 2022;62(1). DOI: 10.18087/cardio.2022.1.n1695